

Search for Right-Handed Currents in the Decay Chain $K^+ \rightarrow \mu^+ \nu$, $\mu^+ \rightarrow e^+ \nu \bar{\nu}$

J. Imazato, Y. Kawashima,^(a) K. H. Tanaka, and M. Takasaki

National Laboratory for High Energy Physics (KEK), Tsukuba-shi, Ibaraki-ken 305, Japan

M. Aoki and T. Yamazaki

Institute for Nuclear Study, University of Tokyo, Tanashi-shi, Tokyo 188, Japan

R. S. Hayano, M. Iwasaki, H. Outa,^(b) E. Takada,^(c) and H. Tamura

Department of Physics and Meson Science Laboratory, University of Tokyo, Bunkyo-ku, Tokyo 113, Japan

(Received 5 May 1992)

Positron asymmetry in the decay of muons produced in $K^+ \rightarrow \mu^+ \nu$ has been precisely measured in a search for right-handed currents. A novel technique utilizing a “ $K_{\mu 2}$ muon beam” from the at-rest decay of positive kaons in a primary-proton-beam target was employed. A limit of $|\xi P_\mu| > 0.990$ (90% C.L.) was obtained from the energy-integrated positron asymmetry observed in muon spin precession under a transverse magnetic field. This limit sets a new constraint on the mass of a second weak boson (M_{W_2}) as well as on the Cabibbo angle of the right-handed sector.

PACS numbers: 13.20.Eb, 12.15.Cc, 13.35.+s, 14.60.Ef

In the left-right symmetric model of the weak interaction [1], the second weak boson (W_2), which is predominantly right handed ($W_2 = W_L \sin \zeta + W_R \cos \zeta$, $|\zeta| \ll 1$; here W_L and W_R are the boson weak eigenstates and ζ is the mixing angle), acquires a much heavier mass than does the predominantly left-handed boson W_1 ($W_1 = W_L \cos \zeta - W_R \sin \zeta$), suppressing a right-handed current (RHC). Experimental searches for RHC's have recently been pursued for a number of processes with very high precision [2]. Among them, the muon-decay positron asymmetry measurement stands out as being one of the most stringent data if the right-handed neutrino is not heavy, and RHC decay is kinematically allowed, since it can simultaneously constrain both the square of the mass ratio $\epsilon = (M_{W_1}/M_{W_2})^2$ and ζ with high sensitivity.

At TRIUMF the positron asymmetry at the spectrum end point in μ^+ decay has been measured using surface muon beams from π^+ decay [3,4], giving a limit of $|\xi P_\mu \delta / \rho| > 0.99682$. Here, P_μ is the μ spin polarization; ξ , δ , and ρ are the Michel parameters. They concluded that $M_{W_2} > 482$ GeV for $\zeta = 0$, and that $|\zeta| < 0.040$ for $M_{W_2} = \infty$ under the assumption that the Cabibbo angle for the right-handed sector (θ_R) is the same as for the left-handed sector (θ_L). The positron asymmetry integrated over energy has also been measured at the Paul Scherrer Institute to be $\xi P_\mu = 1.0027 \pm 0.0084$ [5].

In general, however, it is a totally open question whether the hitherto unknown Cabibbo angle for the right-handed sector (θ_R) is equal to or different from the known θ_L ; a class of models which allow $\theta_R \neq \theta_L$ is argued [6,7]. The strangeness-changing $K_{\mu 2}$ decay chain, $K^+ \rightarrow \mu^+ \nu$, $\mu^+ \rightarrow e^+ \nu \bar{\nu}$, can then provide information from an orthogonal direction [8]. The deviation of $|\xi P_\mu|$ from unity can be expressed as $1 - |\xi P_\mu| = 2(\epsilon \sin \theta_R / \sin \theta_L + \zeta)^2 + 2(\epsilon^2 + \zeta^2)$; for the $\pi_{\mu 2}$ decay chain it is $2(\epsilon \cos \theta_R / \cos \theta_L + \zeta)^2 + 2(\epsilon^2 + \zeta^2)$ [9]. Thus, the $K_{\mu 2}$ de-

cay chain might have a higher sensitivity to ϵ if θ_R is large. Kaon experiments, however, are subject to the available lower beam intensity. In fact, in the results of the best previous experiment, $\xi P_\mu = -0.97 \pm 0.047$ [8,10] was limited by a rather large statistical error.

In this Letter, we report on a new measurement of ξP_μ in a $K_{\mu 2}$ decay chain performed at the KEK 12-GeV proton synchrotron by means of a novel technique involving a “ $K_{\mu 2}$ muon beam” [11], yielding a drastically improved experimental limit. A thin platinum target was bombarded with protons, and a μ^+ beam with a momentum of about 235 MeV/c from the stopped K^+ decay in the target was transported as a monochromatic beam with a high-resolution beam line constructed for this experiment. Thus, a high-flux μ^+ beam was realized, which, analogous to the “surface muon beam” in the case of $\pi_{\mu 2}$, should have $|P_\mu| = 1.0$ without an RHC admixture. The positron asymmetry was precisely measured by stopping this beam using the transverse-field muon-spin-rotation method.

Muons in the beam were discriminated from pions and positrons using differences in the time of flight as well as the stopping range. In order to reject a scattered beam in the channel, which might be depolarized, each beam particle was tracked using two drift chambers and a slit counter at an intermediate focus. The muon momentum spectrum was measured by sweeping the channel magnet settings (Fig. 1) producing a spectacular peak at 233 MeV/c. (There is a shift of about 2.5 MeV/c due to energy loss in the target.) Although there was a small amount of background under the peak due to pion decay in flight, its influence could be corrected.

Incident muons had to be slowed down through a degrader (graphite) of smaller atomic number in order to avoid excessive spin depolarization; they were then stopped in an aluminum target (Fig. 2). The incident an-

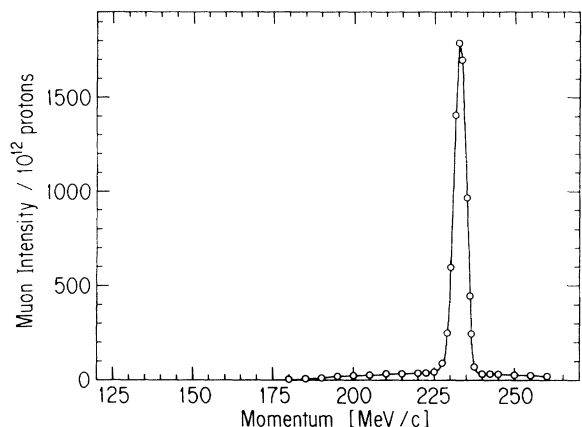


FIG. 1. Momentum spectrum of the muon beam observed by sweeping the channel settings. The flat component under the peak stems from the decay in flight of pions.

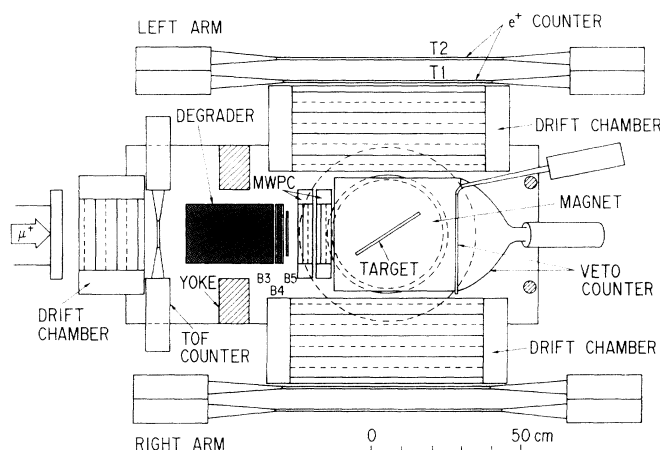


FIG. 2. Plan view of the experiment. The magnetic field (105 G) at the target is vertical.

gle in front of the graphite was measured with a drift chamber comprising four x and y layers. Two multiwire proportional chambers (MWPC's) tracked the trajectory after the graphite, producing information concerning multiple scattering, while contributing to the stopping-point determination. The target was an annealed Al plate with a purity better than 0.99999 and a thickness of 3 or 5 mm, which should have neither initial loss nor relaxation of polarization. It was placed in a helium-gas bag in a magnet gap of 20 cm tilted by 34° from the beam axis; muon stopping efficiency was 34% and 53% for the 3- and 5-mm targets, respectively.

The target was surrounded by three veto counters: two on the magnet pole pieces and one behind the target. These counters functioned so as to identify μ^+ stopping, to reject background events, and to monitor pileup events. A vertical magnetic field of 105 G at the target center was applied with an iron-core magnet. Decay positrons were detected on the left- and right-hand sides with a total solid angle of 5% of 4π sr. Each arm comprised counters T1 and T2 and a drift chamber with four horizontal and four vertical wire layers. Positrons from nearly zero to the maximum energy (52.8 MeV) were accepted. The time between the incident beam and the positron signal (defined by T2) was recorded up to 16 μ s.

Measurements were performed under several different conditions in order to determine the consistency of the data: a peak momentum of 233 MeV/c with the 3-mm target (run 1), the 5-mm target (run 2), the 5-mm target with an additional 10-mm-thick Al absorber between T1 and T2 (run 3), and at ± 1.8 MeV/c off peak with the 3-mm target (runs 4 and 5, respectively). For correcting the π^+ -origin μ^+ background lying under the peak, the asymmetry was also measured in the background region off the peak (run 6-10 for 215, 220, 225, 240, and 245 MeV, respectively).

The positron time spectrum was generated according to the following procedure. First, a muon decay point was

determined from μ^+ tracking onto the target. Muons stopping in the material near the magnet pole pieces were rejected. A cut was then imposed on the goodness of e^+ tracking. Only events with at least three hits in each of the x and y planes were analyzed. Events were further selected from decays in a fiducial thickness of $|t| < 5.0$ cm along the target plane. The lack of bias present in these three cuts was assured by the integral and differential dependence of the asymmetry upon the cut parameters. Figure 3 shows the obtained positron time spectra of run 1, which exhibits oscillation of 1.42 MHz.

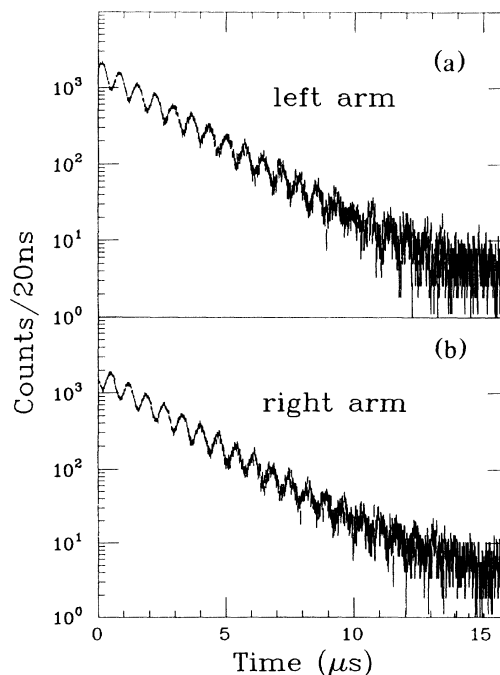


FIG. 3. Typical raw time spectra of e^+ (from run 1) by the (a) left-hand-side and (b) right-hand-side arms. In these spectra, the emission angle in each arm is not yet corrected.

TABLE I. Positron asymmetry and ξP_μ . A_{obs} is the fitted asymmetry and A_{corr} is the value after the corrections described in text. ξP_μ was derived by applying corrections of μ^+ polarization to $-3A_{\text{corr}}$. In the parentheses statistical and systematic errors are indicated. Momentum has a shift of about 2.5 MeV/c due to energy loss in the target.

Run	Momentum (MeV/c)	Target	Analyzed events	A_{obs}	A_{corr}	ξP_μ
1	233.0	3 mm thick	379 489	0.3237(26)	0.3354(26)(20)	-1.0079(78)(60)
2	233.0	5 mm thick	740 154	0.3146(18)	0.3321(18)(21)	-0.9980(54)(64)
3	233.0	5 mm with absorber	679 737	0.3348(19)	0.3329(19)(15)	-1.0004(57)(46)
4	231.2	3 mm thick	228 453	0.3246(33)	0.3380(33)(21)	-1.0157(99)(62)
5	234.8	3 mm thick	302 344	0.3177(28)	0.3301(28)(20)	-0.9920(84)(60)

The left- and right-hand arms have opposite phases. One could follow an exponential decay up to 16 μs , the constant background being at a level of 10^{-3} . The spectra of the other runs were similar; they were fitted after correcting for each e^+ emission angle in the horizontal spin precession plane, using

$$\frac{d^2N}{d\Omega dt} = N_0 \exp\left(-\frac{t}{\tau_\mu}\right) \{1 + \alpha G(t) A \cos(\omega t + \phi)\} + B, \quad (1)$$

and using N_0 , τ_μ , A , ω , ϕ , and B as free parameters. Here, τ_μ is the muon lifetime, $A = \xi P_\mu/3$ the asymmetry coefficient, ω the central frequency, ϕ the initial emission angle, and B the constant background. The attenuation factor ($\alpha = 0.9922$) due to the finite vertical acceptance and damping function [$G(t)$] due to the field inhomogeneity were experimentally determined from the event distribution. The results of the fitting are summarized in Table I.

The asymmetry of the background, which originated mostly from the forward decay of pions in flight, had the same sign and the precession phase. Since there was no significant momentum dependence within the statistical accuracy, its contribution was subtracted using a mean value of $A_{\text{BG}} = 0.233 \pm 0.016$ from runs 6–10. It gave a correction of $\delta A = (A_{\text{obs}} - A_{\text{BG}})/r$ with rather small uncertainty, where r is the background to the signal ratio. The observed asymmetry was also affected by the interactions of e^+ in the Al target, as well as in the absorber (run 3). These are (1) the absorption of low-energy e^+ , (2) angular attenuation due to multiple scattering and Bhabha scattering, (3) in-flight annihilation, (4) admixture of knockon e^- from the target, and (5) event rejection by detecting a knockon e^- in a veto counter. They were evaluated by a simulation calculation using the EGS4 code [12], which gave $\delta A = +0.0136 \pm 0.0018$ for the 5-mm target and $+0.0075 \pm 0.0016$ for the 3-mm target; the Al absorber run was also simulated to be -0.0056 ± 0.0010 . The μ^+ radiative decay was calculated according to Kinoshita and Sirlin [13] to give $\delta A = +0.00089$ (runs 1, 2, 4, and 5) and $+0.00068$ (run 3). Other corrections to A , such as the effect of finite time bin of 10 ns ($+0.0001$), the distortion of positron orbit in

the field region (< 0.0003), and the effect of the inefficiency of the drift chambers (-0.0004), were evaluated to be small. These δA corrections were applied to A_{obs} to give A_{corr} in Table I.

Depolarization of μ^+ due to multiple scattering through the material in the beam line was well understood [14]; those from the Pt target ($\delta P_\mu = 0.05\%$), the graphite degrader (0.08%), and the Al target (0.03%) are significant. The spin-flip probability through the interaction with electrons in matter in the beam line was evaluated to be negligibly small. The effect of muon trajectory distortion in the magnetic field after the tracking chambers is 0.01%. Since the channel accepted muons with a 1.2% momentum bite, the radiative decay $K^+ \rightarrow \mu^+ \nu \gamma$ was admixed. An upper limit of its contribution was estimated to be 0.02% using an expression given in Ref. [15].

Correcting for all of these effects, the results of ξP_μ are listed in Table I. Since there is no significant difference in the results among the five conditions, all of the five

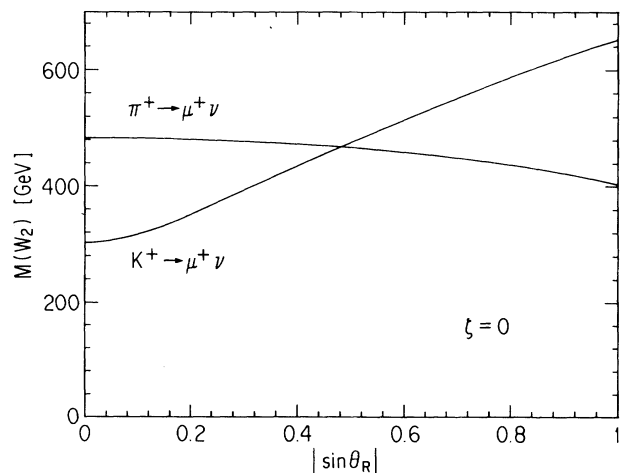


FIG. 4. Mass limit of the 90% C.L. for the second weak boson (W_2) in the special case of a mixing angle of $\zeta = 10$. The lines are the result from ξP_μ of this K^+ decay experiment, and the result from $\xi P_\mu \delta/\rho$ of π^+ decay [3]; here, $\delta = \rho = \frac{1}{4}$ was assumed and the values $M_{W_1} = 80.6$ GeV and $\sin\theta_L = 0.221$ were taken.

data could be averaged so as to improve the statistical accuracy, giving

$$\xi P_\mu = -1.0013 \pm 0.0030(\text{stat}) \pm 0.0053(\text{syst}). \quad (2)$$

The main systematic errors are all associated with the above-mentioned corrections. The uncertainty in positron-scattering corrections is dominant, especially regarding evaluation of the e^- knockon process. The ambiguities of the analysis parameters, such as the e^+ tracking goodness cut, were also included in the systematic error. By adding the statistical and systematic errors quadratically, the 90% C.L. limit was set to be $|\xi P_\mu| > 0.990$. The corresponding M_{W_2} limit for a special case of $\zeta=0$ is shown in Fig. 4 as a function of $|\sin\theta_R|$. Although the constraint is weaker (303 GeV) for the small- $|\sin\theta_R|$ regime, it supersedes the $\pi_{\mu 2}$ data for large $|\sin\theta_R|$. In fact, the limit of M_{W_2} at $|\sin\theta_R|=1$ amounts to 653 GeV.

The authors are thankful to Professor H. Sugawara, Professor K. Nakai, and Professor S. Iwata for their encouragement and discussions. They are indebted to Professor Y. Shimizu for helpful discussions concerning spin-flip scattering processes.

^(a)Present address: Institute for Physical and Chemical Research, Wako-shi, Saitama 351-01, Japan.

^(b)Present address: Institute for Nuclear Study, University of Tokyo, Tokyo, Japan.

^(c)Present address: National Institute of Radiological Sci-

ences, Inage-ku, Chiba-shi, Chiba 263, Japan.

- [1] J. C. Pati and A. Salam, *Phys. Rev. D* **10**, 275 (1974); R. N. Mohapatra and J. C. Pati, *Phys. Rev. D* **11**, 566 (1975).
- [2] A. S. Carnoy *et al.*, *Phys. Rev. Lett.* **65**, 3249 (1990); D. Dubbers, W. Mampe, and J. Döhner, *Europhys. Lett.* **11**, 195 (1990).
- [3] A. Jodidio *et al.*, *Phys. Rev. D* **34**, 1967 (1986); **37**, 237(E) (1988).
- [4] D. P. Stoker *et al.*, *Phys. Rev. Lett.* **54**, 1887 (1985).
- [5] I. Beltrami *et al.*, *Phys. Lett. B* **194**, 326 (1987).
- [6] P. Herczeg, *Phys. Rev. D* **34**, 3449 (1986).
- [7] P. Langacker and S. U. Sankar, *Phys. Rev. D* **40**, 1569 (1989).
- [8] R. S. Hayano *et al.*, *Phys. Rev. Lett.* **52**, 329 (1984).
- [9] The expression for $\pi_{\mu 2}$ can be derived from Ref. [6] with the assumptions of $g_R=g_L$, and that the CP -violating phases α and ω are zero. For $K_{\mu 2}$, P_μ has been given in T. Oka, *Phys. Rev. Lett.* **50**, 1423 (1983).
- [10] T. Yamanaka *et al.*, *Phys. Rev. D* **34**, 85 (1986).
- [11] K. H. Tanaka *et al.*, *Nucl. Instrum. Methods Phys. Res., Sect. A* **316**, 134 (1992).
- [12] W. R. Nelson, H. Hirayama, and D. W. O. Rogers, Stanford Linear Accelerator Center Reports No. SLAC-265 (unpublished) and No. UC-32, 1985 (unpublished).
- [13] T. Kinoshita and A. Sirlin, *Phys. Rev.* **107**, 593 (1957); **113**, 1652 (1959).
- [14] V. L. Lyuboshits, *Yad. Fiz.* **32**, 702 (1980) [*Sov. J. Nucl. Phys.* **31**, 509 (1980)].
- [15] D. Yu. Bardin and S. M. Bilen'kii, *Yad. Fiz.* **16**, 557 (1972) [*Sov. J. Nucl. Phys.* **16**, 311 (1973)].

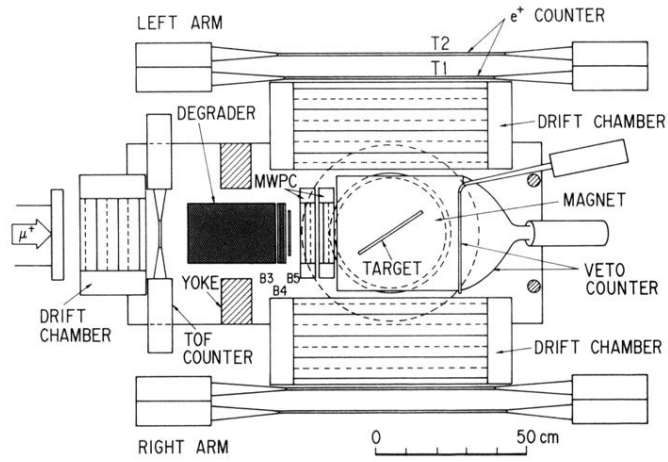


FIG. 2. Plan view of the experiment. The magnetic field (105 G) at the target is vertical.